Published in final edited form as:
Nature. 2020 January ; 577(7790): 376–380. doi:10.1038/s41586-019-1864-1.

A sensory appendage protein protects malaria vectors from pyrethroids

V A Ingham, **A Anthousi**
Vector Biology, Liverpool School of Tropical Medicine, Pembroke Place, Liverpool, L3 5QA, UK

V Douris,
Foundation for Research and Technology - Hellas (FORTH), Institute of Molecular Biology and Biotechnology, Nikolaou Plastira 100, Vassilika Vouton, GR - 700 13 Heraklion, Crete, Greece

N J Harding
The Big Data Institute, University of Oxford, Old Road Campus, Oxford, OX37LF

G Lycett, **M Morris**
Vector Biology, Liverpool School of Tropical Medicine, Pembroke Place, Liverpool, L3 5QA, UK

J Vontas,
Foundation for Research and Technology - Hellas (FORTH), Institute of Molecular Biology and Biotechnology, Nikolaou Plastira 100, Vassilika Vouton, GR - 700 13 Heraklion, Crete, Greece; Pesticide Science Laboratory, Department of Crop Science, Agricultural University of Athens, 11855 Athens, Greece

H Ranson
Vector Biology, Liverpool School of Tropical Medicine, Pembroke Place, Liverpool, L3 5QA, UK

Summary

Pyrethroid-impregnated bednets have driven significant reductions in malaria morbidity and mortality in Africa since the beginning of the century [1]. The intense selection pressure exerted by bednets has precipitated widespread and escalating pyrethroid resistance in African *Anopheles* populations, threatening to reverse gains made by malaria control [2]. Here we show that a leg-enriched sensory appendage protein, *SAP2*, confers pyrethroid resistance in *Anopheles gambiae*. *SAP2* expression is elevated in insecticide-resistant populations and is further induced upon

Correspondence and requests for material should be addressed to hilary.ranson@lstmed.ac.uk or victoria.ingham@lstmed.ac.uk.

Author contribution
V.I. and H.R conceived the experimental design. V.I performed: all transcriptomic expression experiments; RNAi and phenotyping; data analysis, PCR and associated sequencing. A.A and G.L produced the transgenic lines and associated phenotypic characterisation. V.D and J.V performed the binding assays and associated protein expression experiments. N.H analysed the 1000 genomes data and produced the haplotype SNP panel. M.M provided all insectary support. V.I and H.R drafted the manuscript.

Data Availability
All data analysed during this current study are available on public repositories and detailed in the present paper, or in the Extended Data files, or are available from the authors upon request.

The authors declare that they have no competing interests.

Europe PMC Funders Author Manuscripts

mosquito contact with pyrethroids. *SAP2* silencing fully restores mosquito mortality, whilst its overexpression results in increased resistance, likely due to the high-affinity *SAP2* binding to pyrethroid insecticides. Mining of genome sequence data reveals a selective sweep near the *SAP2* locus in three West African countries, with the observed increase in haplotype associated SNPs mirroring increasing resistance reported in Burkina Faso. Our study identifies a new insecticide resistance mechanism that is likely highly relevant to malaria control efforts.

Background

Anopheline mosquitoes are the only genus capable of transmitting human malaria. Targeting the mosquito has proven to be the most effective means of reducing the incidence of malaria, and the massive scale up of insecticide-based interventions, most notably long-lasting insecticidal nets (LLINs), has driven the dramatic reductions in malaria cases in Africa in the 21st century [1]. However, worryingly, after many years of progress, gains in malaria control are now stalling, with an estimated 219 million cases and 435 000 malaria associated deaths across Africa in 2017 prompting a re-examination of the effectiveness of the primary prevention tools [2]. LLINs have proven so effective in preventing malaria because they not only provide personal protection to LLIN users by reducing biting by the night feeding *Anopheles* mosquitoes, but they also have a community effect, whereby contact with the insecticide decreases the likelihood that mosquitoes will survive long enough for the *Plasmodium* parasite development and transmission [3]. The scale up of LLINs has exerted intense selection pressure on *Anopheles* vectors to develop resistance to pyrethroids, the insecticide class used to treat all LLINs, and as a result, the community effect of LLINs is being eroded [4]. To mitigate against catastrophic failure of insecticide-based vector control tools, the resistance mechanisms must be identified and targeted. Successful management of insecticide resistance has been demonstrated by trials of pyrethroid nets containing the synergist piperonyl butoxide (PBO) [5], a potent inhibitor of metabolic resistance caused by cytochrome P450s, one of the most widespread, and hitherto most potent, resistance mechanisms [6,7]. By blocking this resistance mechanism, PBO-pyrethroid nets restore insecticide susceptibility, leading to a reduction in malaria cases in areas where metabolic resistance prevails [5].

Although PBO-pyrethroid nets are now replacing standard pyrethroid-only nets in many sites across Africa [8], not all pyrethroid resistant populations can be effectively targeted by this synergist [8,9] as additional mechanisms are contributing to the resistance phenotype. Recently, using a meta-analysis approach of transcriptomic data from pyrethroid resistant *An. gambiae* populations from across Africa, we identified multiple new resistance mechanisms, including up-regulation of putative insecticide binding proteins [10]. By screening this transcriptomic data from Burkina Faso and Côte d'Ivoire, areas with particularly high pyrethroid resistance and low PBO synergism [9,11], we found that one family of binding proteins, the sensory appendage proteins, were particularly highly overexpressed in these populations (Extended Data Table 1).

Sensory appendage proteins are members of the chemosensory protein (CSP) family, small soluble proteins found only in arthropods [12] that function in the transport of hydrophobic

Europe PMC Funders Author Manuscripts

compounds through the sensillum lymph [13]. Eight CSP genes are present in the genome of *Anopheles gambiae* seven of which are clustered on chromosome 3R (Extended Data Figure 1). Four members of this family have previously been expressed *in vitro* and shown to bind aromatic compounds [14]. Members of the CSP family have been shown to be induced by insecticide exposure, for example by avermectin in the silkworm *Bombyx mori* [15], pyrethroids in the diamondback moth *Putella xylostella* [16] and noenicitinoids in the whitefly *Bemiscia tabaci* [17].

CSP expression and localisation

To determine whether elevated CSP expression was associated with pyrethroid resistance in *An. gambiae* we characterised the expression of all eight members of the family in females of a multi-resistant laboratory colony originally from Côte d'Ivoire (Tiassalé). We observed two CSPs, *SAP2* (AGAP008052) and *CSP6* (AGAP001303), with significantly higher constitutive expression when compared to two separate susceptible controls (Extended Data Figure 2). We next determined localisation of CSP expression in multiple tissues, including body areas that are the primary points of mosquito contact with LLINs: the legs, head and antennae; the major detoxification tissues: the Malpighian tubules and the midgut; the reproductive tissues; and remaining abdominal carcass (Figure 1A). Six of the eight CSPs, including both *SAP2* and *CSP6,* were enriched in the legs in both *Anopheles* populations, two of the CSPs were enriched in the head (*SAP2* and *SAP3* (AGAP008054)); two in the antennae (*CSP3* (AGAP008055) and *CSP5* (AGAP008058)) and one in the abdomen carcass (*CSP1* (AGAP008059)).

We performed a time course to determine whether any of the eight CSPs were induced by exposure to pyrethroids in the resistant strain (Figure 1B; Extended Data Figure 3a) and found that four of the eight CSPs were significantly induced by deltamethrin, the pyrethroid most widely used in LLINs, including the constitutively overexpressed *SAP2* and *CSP6*, in addition to *SAP3* and *CSP4* (AGAP008062) (Figure 1B). Examining the tissue specificity of the induction 4-hours post-exposure showed *SAP2, SAP1* (AGAP008051) and *CSP3* as induced in multiple tissues, including the legs, whilst *CSP4*, *CSP6* and *CSP1* show induction in a single tissue (Figure 1C; Extended Data Figure 3B).

Evidence CSPs confer resistance

Having established that CSPs are highly overexpressed in the appendages of pyrethroid resistant mosquitoes, and expression of a subset of this family is further induced by insecticide exposure, we next performed RNAi silencing of these CSPs (Extended Data Figure 4) in females from the highly pyrethroid resistant Tiassalé colony before exposing them to a panel of insecticide classes (pyrethroids, carbamates and organophosphates) widely used in public health. Strikingly, *SAP2* silencing almost completely restored susceptibility to the pyrethroid deltamethrin, whilst also significantly increasing the susceptibility to the other two pyrethroids permethrin and α-cypermethrin used in these analyses (Figure 2A). No change in mortality was observed after exposure to the other insecticide classes, indicating pyrethroid specificity of the mechanism. We further explored this striking phenotype in a second multi-resistant population from Burkina Faso (Banfora)

and again found mortality was significantly restored after exposure to deltamethrin (Figure 2A). Knock down of the other three CSPs had no effect on mortality to any insecticide class, except in the case of *CSP6* knockdown which also significantly increased susceptibility to deltamethrin in Tiassalé mosquitoes, although not to the same extent as *SAP2* (Extended Data Figure 5). Conversely, over-expression of *SAP2* in an insecticide susceptible population (Extended Data Figure 6) significantly increased pyrethroid resistance, directly linking the function of this protein to insecticide resistance (Figure 2B). To check for adverse changes to the life history traits due to disrupting *SAP2* expression, we recorded the survivorship, blood feeding ability and egg production in dsSAP2 injected females and found no significant changes compared to a GFP-injected control, indicating the mortality observed is due to a direct effect of *SAP2* on the insecticide and not reduced overall fitness (Extended Data Figure 7).

To determine a putative mode of action whereby a chemosensory protein could confer resistance, we next investigated whether these proteins act as pyrethroid binding proteins. We heterologously expressed *SAP2* and two closely related CSPs (*SAP1* and *SAP3*) in *E. coli* and carried out competitive binding assays with the fluorescent marker N-phenyl-1-naphthylamine and a panel of insecticides (Figure 2C). *SAP2* bound to all three pyrethroid insecticides tested: deltamethrin (IC_{50} = 3.99μM); permethrin (IC_{50} = 4.77μM); and α-cypermethrin (IC_{50} = 3.74μM) but did not bind pirimiphos-methyl (organophosphate) or bendiocarb (a carbamate). The IC_{50} values were similar to those found for the most important cytochrome p450s responsible for metabolic clearance of pyrethroid insecticides [6,7] (deltamethrin $IC_{50,\ CYP6M2;\ CYP6P3}$ = 4.24μM; 3.17 μM, permethrin $IC_{50,\ CYP6M2;\ CYP6P3}$ = 8.07μM; 6.77μM [18]). The binding of the pyrethroids to *SAP2* had significantly higher specificity ($p_{ANOVA} < 0.0001$) than the other *SAP* proteins; however, both *SAP1* and *SAP3* bound weakly to deltamethrin (IC_{50} > 10μM) and *SAP1* moderately to α-cypermethrin (IC_{50} = 9.02μM).

Having established the importance of *SAP2* to pyrethroid resistance in a lab setting, and detected the over-expression of this transcript in available transcriptomic data from multiple resistant West African field populations (Figure 3A; Extended Data Table 1), we next looked for any evidence of selection at this locus, utilising data from the *An. gambiae* 1000 genomes project [19] and further *de novo* sequencing. We computed the selection statistics iHS [20] and XPEHH [21] from 1142 wild caught *An. gambiae* [19] in the region surrounding the CSP cluster on chromosome 3R (Figure 3B). Evidence for a selective sweep at this locus was observed in *An. gambiae* from Guinea and Burkina Faso. The swept haplotype is present at low frequency but there is evidence of haplotype sharing between Guinea, Burkina Faso and Cameroon. We next identified SNPs diagnostic of the derived haplotype in this selective sweep (Figure 3B) and sequenced this region in individual mosquitoes collected from the Banfora region of Burkina Faso from 2011 to 2018. This haplotype was stable in frequency in *An. gambiae* s.s., indicating that this sweep occurred before the Anopheles 1000 genomes collections in 2012 and pre-dating our collection dates (Figure 3C; Supplementary Table 1). Conversely, *An. coluzzii* samples collected from 2011 to 2018 showed a large increase in frequency of the SNPs associated with the sweep (Figure 3C; Supplementary Table 1) and this corresponded with a sharp increase in the prevalence of pyrethroid resistance occurring over this time period (Extended Data Figure 8).

Discussion

Our results show that *SAP2*, a chemosensory protein with no previous known function in insecticide resistance, has a key role in conferring pyrethroid resistance in the *An. gambiae* species complex via the binding of insecticides at the first point of mosquito contact with bednets. When elevated *SAP2* expression was introduced into an otherwise susceptible background, the transgenic line was more resistant to pyrethroids but the phenotype was less dramatic than seen in the *SAP2* knock down lines, perhaps indicating that *SAP2* acts in conjunction with other resistance mechanism to provide an additive effect. Given its strong binding to pyrethroid insecticides, it is possible that *SAP2* acts by sequestering the insecticide directly, thereby either preventing insecticide function on the nervous system or facilitating its detoxification. Crucially, longitudinal sequencing of field samples and available transcriptomic data from wild collections show that this mechanism is being selected for in multiple countries in West Africa, highlighting its relevance in field settings. Nationwide distribution of LLINs has not impacted malaria transmission in Burkina Faso, where cases continue to rise annually [22]. Our finding of a potent new mechanism that has rapidly swept across Anopheline populations in this region will help address the contribution of insecticide resistance to the persistence of malaria, while the identification of the corresponding SNPs will facilitate tracking its spread. Finally, the identification of this novel insecticide sequestration mechanism offers the concrete possibility to restore the effectiveness of pyrethroid insecticides in natural mosquito populations through identifying new targets for inhibitors for bed net incorporation, in an analogous manner to the incorporation of PBO into nets, a factor that may prove critical in the path to malaria elimination across Africa.

Methods

Mosquito strains

The populations, each belonging to *An. gambiae* species complex, used in these experiments were reared and maintained at the Liverpool School of Tropical Medicine (LSTM), under standard insectary conditions at 27°C, 70-80% humidity, under a 12:12 hour photoperiod. Both the Tiassalé (*An. gambiae* s.l.) strain from Côte D'Ivoire [11], and the Banfora strain (*An. coluzzii*) from Burkina Faso [24] are insecticide resistant populations and have been maintained under insecticide pressure since colonisation in 2009 and 2014 respectively. The lab susceptible populations N'Gousso (*An. coluzzii*) [25], Kisumu (*An. gambiae s.s.*) and G3 (*An. gambiae s.l.*) originate from Cameroon, Kenya and The Gambia respectively. *An. gambiae* s.l. here refers to a mixture of *An. gambiae* and *An. coluzzii*.

RNAi

PCR was performed on Tiassalé cDNA using Phusion® High-Fidelity DNA Polymerase (Thermo Scientific, UK) following manufacturer's instructions and primer sets with a T7 docking sequence at the 5' end of both the sense and antisense primers. Primers were designed using NCBI Primer BLAST to produce an asymmetric product with a length of 300-600bp, a GC content of 20-50% and no more than three consecutive equivalent nucleotides (Supplementary Table 3). PCR was performed with the following cycle: three

minutes 98°c, 35 cycles of seven seconds at 98°c, 7 seconds at calculated T_m and 10 seconds at 72°c, with a final hold at 72°c for seven minutes. PCR products were purified using a Qiagen QIAquick PCR Purification kit following manufacturer's instructions. dsRNA was synthesised using a Megascript® T7 Transcription (Ambion, UK) kit, with a 16-hour 37°c incubation, following manufacturer's instructions. The dsRNA was cleaned using a MegaClear® Transcription Clear Up (Ambion, UK) kit, with nuclease free DEPC water, twice heated at 65°c for 10 minutes, to elute the sample. The resultant dsRNA product was analysed using a nanodrop spectrometer (Nanodrop Technologies, UK) and subsequently concentrated to 3μg/μl using a vacuum centrifuge at 37°c. Three-to-five day old, presumed mated, non-blood fed females, were immobilised on a CO_2 block and 69nl dsRNA injected directly into the thorax, between the cuticle plates of the abdomen, underneath the wing. As a control, non-endogenous GFP dsRNA was injected at the same amount and concentration.

UAS-SAP2 Plasmid Construction

Due to difficulty in transformation of a UAS-SAP2 construct into *E. coli* with a complete ORF, a fusion gene was created that was interrupted by a synthetic intron directly after the start codon. Two fragments were amplified separately and fused together through 40bp overlapping nucleotides (20 final nucleotides of synthetic intron and 20 nucleotides downstream the SAP2 start codon). The 5' fragment containing a start codon, intron and SAP2 overlap was amplified from pSL-attB-Gyp-UAS14i-Cyp6P3-eYFP (Adolfi A. and Lycett G., unpublished). In parallel, *SAP2* was amplified from Tiassalé genomic DNA using primers F-TTCTGAATTCCATCATGAAACTGTTCGTCGCC and R-TTCTCTCGAGTTATTCCAGCTTGATG. The 3' fragment for fusion was amplified from the SAP2 PCR product with the overlapping sequences indicated above. The primers used were F-TTCTGAATTCCATCATGGTAAGTATCAAGGTTACA, R-GCGATGGCGACGAACAGTTTCTGTGGAGAGAAAGGCAAAG and F-CTTTGCCTTTCTCTCCACAGAAACTGTTCGTCGCCATCGC, R-TTCTCTCGAGTTATTCCAGCTTGATG, respectively. The two fragments were fused together by PCR using the outer amplification primers, sub-cloned into pJET1.2 (Thermo Scientific) and inserted into pSL-attB-Gyp-UAS14-eYFP-gyp-attB (Lycett G., unpublished), which carries inverse attB site for RCME flanking, the 3xP3-YFP transformation marker and multiple cloning site through the EcoRI/XhoI restrictions sites, to generate plasmid pUAS-SAP2. Sequence analysis indicated a point mutation within the synthetic intron but outside of the splice and acceptor donor sites.

Transgenic Lines

The CFP marked A10 Ubi-GAL4 line [26] was used as the RCME docking line to establish the UAS:SAP2 line. The A10 promoter, *polyubiquitin c* (PUBc), has been previously characterised, and shows high levels of expression throughout adult male and female mosquitoes[26]. mCherry under the PUBc promoter in the A10 line has fluorescence in the thorax, non-sclerotised abdomen, appendages (wing veins, antennae, palps, proboscis/labium and legs) [26] (Extended Data Figure 6b). Microinjections were performed on approximately 200 embryos with 350ng/μl of SAP2:UAS responder plasmid and 150ng/μl of phiC31 integrase helper plasmid pKC40 (gift from L. Ringrose, Humboldt University Berlin). 38 F_0 L1 larvae transiently expressing the YFP marker were obtained, reared

separately and crossed into opposite sex G3. Three YFP positive F_1 male adults were identified from screening, that were backcrossed with wild-type G3, and characterised for orientation of exchange cassette through a diagnostic PCR. All males showed identical orientation in the expected genomic site. From these F_1 crosses, a single isofemale line was selected, that showed expected 50% YFP inheritance in F_2. This line was further characterised after crossing with the parental A10 Ubi-Gal4 driver line for correct splicing of the inserted intron (Extended Data Figure 6c) and for insecticide bioassays.

Bioassays

72-hours post injection, 3-5-day old adult females were exposed to a panel of insecticides using standard insecticide impregnated papers in WHO tubes [27]. In each case, 15-30 adult females were exposed to insecticide for 1-hour and then left in a control tube for 24 hours in insectary conditions before mortality was scored (minimum biological replicates = 3; maximum = 17). For each experiment, mosquitoes were simultaneously exposed to untreated control papers. GFP-injected mosquitoes were used as controls for the RNAi bioassays and the GAL4-driver line acted as a control for the bioassays on the transgenic strains. For the induction experiments, no 24-hour recovery period was allowed, and mosquitoes were taken at the time point directly after 1-hour exposure; this experiment was only possible on the resistant population due to mortality in the susceptible control. Bartlett and Shapiro tests were used to confirm homogeneity of variance and normality of data respectively. For non-normal data transformations were performed to achieve normality. Analysis of mortality data was done using an ANOVA test followed by a Tukey *post hoc* test. Graphs were produced using GraphPad Prism 8.0.2 (La Jolla California USA, www.graphpad.com). Mortalities and significance levels for figure panels are shown in Supplementary Data Table 2.

RNA Extraction

RNA was extracted and purified in each experimental set using an Arcturus PicoPure RNA Isolation Kit (Thermo Fisher, UK) following manufacturer's instructions. Whole body resistant and susceptible experiments, and RNAi knockdown efficiency checks, used five to seven, 3-5-day old adult female mosquitoes, ground and boiled in extraction buffer. For insecticide induction mosquitoes were snap frozen pre-exposure and at 30 minutes, 1 hour, 2 hours, 4 hours, 24 hours and 48 hours post-deltamethrin exposure of 3-5-day old female mosquitoes and RNA extracted as above. Finally, for tissue experiments; 50-100 3-5-day old females had heads, legs, antennae, midgut, Malpighian tubules, reproductive tissues (and hindgut), along with the remaining abdominal carcass where fat body cells predominate [28], removed with microdissection scissors and tweezers on iced PBS, alongside 5-7 age matched whole females from the same cage. The quality of the RNA was assessed using a nanodrop spectrophotometer (Nanodrop Technologies UK).

qPCR

RNA (1-4μg) from each biological replicate was reverse transcribed using Oligo dT (Invitrogen, UK) and Superscript III (Invitrogen, UK) according to manufacturer's instructions. Quantitative real-time PCR was performed using SYBR Green Supermix III (Applied Biosystems, UK) using an MX3005 and the associated MxPro software v4.10

(Agilent, UK). Primer Blast (NCBI) was used to design primer pairs. Where possible, primers were designed to span an exon junction (Supplementary Table 3). Each 20µl reaction contained 10µl SYBR Green Supermix, 0.3µM of each primer and 1µl of 2ng/µL cDNA. Standard curves for each primer set were used to calculate efficiency, using five 1:5 dilutions of cDNA to ensure that all primer sets met the MIQE guidelines (90-120%). qPCR was performed with the following conditions: 3 minutes at 95°C, with 40 cycles of 10 seconds at 95°C and 10 seconds at 60°C. Relative expression was normalised against two housekeeping genes: EF (AGAP005128) and S7 (AGAP010592). Analysis was performed on $2^{\Delta\Delta Ct}$ values [29]; Bartlett and Shapiro tests were used to confirm homogeneity of variance and normality of data respectively. For non-normal data transformations were performed when possible to achieve normality. Normal data was analysed using an ANOVA followed by Dunnett's *post hoc* test, non-normal data was analysed using Kruskall-Wallis followed by a Dunn's *post hoc* test. Graphs were produced using GraphPad Prism 8.0.2 (La Jolla California USA, www.graphpad.com). All qPCR analysis had three biological replicates and three technical replicates within each biological replicate, with the exception of the transgenics which had two. Relative fold changes and significance levels for each figure panel are shown in Supplementary Data Table 2; primers are shown in Supplementary Data Table 3 and SAP2 sequences to demonstrate conservation of binding site in Extended Data Figure 9. The PCR for sequencing was performed in two reactions, and sequenced using the primers, Region1-F 'CACAACGATTCGTGGTCACC', Region1-R 'CACTTCACAACTTGCAATGAA', sequenced using Region1-R and Region2-F 'TTCATTGCAAGTTGTGAAGTG', Region2-R 'GCACCAGCTGATCGTTGA', sequenced using Region2-F. PCR used Phusion High-Fidelity DNA Polymerase (Thermo Fisher, UK) with a 98°C 30 seconds followed by 40 cycles of 98°C 7 seconds, 64°C for 10 seconds, 72°C for 2 minutes and a final hold of 72°C for ten minutes. Gel extraction used Qiagen Gel Extraction Kit (Qiagen,UK), following manufacturer's instructions and PCR products were Sanger sequenced at Eurofins Genomics, UK.

SAP constructs

SAP1, *SAP2* and *SAP3* proteins were expressed in bacteria (*SAP1* and *SAP3* as N-terminal His-tagged proteins, while *SAP2* which is secreted in the periplasmic space, as a C-terminal His-tagged protein). The bacterial expression constructs used for *SAP1* and *SAP3* expression were generated by directly subcloning the *SAP1* and *SAP3* ORFs (as EcoRI-NdeI fragments) from the relevant constructs used in Iovinella et al. [14] (kindly provided by Alessandra della Torre, Universita "Sapienza", Rome, Italy) into pET16bTeV vector in order to generate plasmids pET16TeV.SAP1 and pET16TeV.SAP3 expressing N-terminal His-tagged versions of SAP1 and SAP3 respectively. For *SAP2* expression, a stepwise cloning strategy into pET22b vector was employed, as follows: *Anopheles gambiae* cDNA (made from RNA from N'Gousso strain mosquito heads) was used as a template for PCR amplification of a 384 bp *SAP2* ORF with Kapa Taq polymerase (Roche, Switzerland) using primers SAP2F: 5'- ATGAAACTGTTCGTCGCCATC-3' and SAP2R: 5'-TTATTCCAGCTTGATGCCCTC-3'under the following conditions: 95°C for 5 min and 30 cycles of 95°C for 30 sec, 60°C for 30 sec and 72°C for 30 sec, followed by a final extension step of 72°C for 5 min. The amplified *SAP2* ORF was subcloned into pGEM-T-Easy vector (Promega) and sequence verified. Plasmid DNA from a positive pGEM.SAP2 clone was

used as template for the amplification of the mature SAP2 ORF (i.e. without the native signal peptide sequence in order to enable cloning in frame to the pET22-encoded bacterial signal peptide), using primers NcoSAP2F: 5'-TAACCATGGCCCAGGAGCAGTACACCACC-3' (to generate an NcoI site in frame with pelB ORF in pET-22b) and XhoSAP2ΔR: 5'-GTCTCGAGTTCCAGCTTGATGCCCTCCTT-3' (to remove the termination codon, thus enabling C-terminal His tagging, and also introduce an XhoI site). The amplified product was digested with NcoI and XhoI and subcloned into the relevant cloning sites of pET-22b. The recombinant plasmid pET22.SAP2His was sequence verified and used for periplasmic protein expression.

Protein expression and purification

Expression of *SAP1* and *SAP3* was carried out in BL21-Codon Plus (DE3) *E. coli* cells (Agilent, UK) harbouring pET16TeV.SAP1 and pET16TeVSAP3 respectively. A single colony was selected and cultured overnight at 37 °C in 80 ml of terrific broth (TB) containing 100μg/mL ampicillin and 34μgr/mL chloraphenicol. The 80ml overnight bacterial culture was used to inoculate a 4L culture of TB containing 100μg/mL ampicillin and 34μg/ml chloramphenicol. Cells were cultured at 37 °C until OD_{595} was equal to 0.8. Recombinant protein expression was induced by addition of 0.4mM isopropyl β-thiogalactopyranose (IPTG) and the bacteria were cultured for additional 4 hours at 30 °C. Bacteria were harvested by centrifugation (5000rpm for 30 min) and the pellet was resuspended in 1M NaCl, 50mM Tris-HCl pH 8.0, 0.2mM EDTA, 0.2mM PMSF buffer and sonicated for 30 min at 4°C. Following sonication, a high-speed centrifugation at 20000xg for 30 min at 4°C, was performed, the supernatant collected and processed to the purification step.

The supernatant containing soluble *SAP1* or *SAP3* was purified by Ni^{2+} affinity chromatography as follows: a 5.5ml Ni-NTA Agarose column was equilibrated with a buffer containing 1M NaCl, 50mM Tris-HCl pH 8.0 and 5mM imidazole. The supernatant was loaded onto the column and washed with equilibration buffer for 10 column volumes (CV). Another wash for 10 column volumes (CV) was performed with 25mM NaCl, 50mM Tris-HCl pH 8.0, 10% glycerol and 10mM imidazole. Bound protein was eluted with 5 CVs of 50mM Tris pH 8.0, 25mM NaCl, 10% glycerol and 300mM imidazole. Fractions with an absorbance at 595 nm (Bradford assay) greater than 3mg/ml were pooled, concentrated and buffer exchanged into 50mM Tris-HCl pH8.0, 25mM NaCl and 10% glycerol with dialysis membrane (6-8 kD) overnight at 4 °C.

For expression of *SAP2*, *E. coli* BL21-Codon Plus (DE3) cells transformed with pET22.SAP2His were cultured overnight at 37°C in 20ml terrific broth (TB) containing 100μg/mL ampicillin and 34μgr/mL chloramphenicol. The 20mL overnight *E. coli* culture was used to inoculate a 2L culture of TB containing 100μg/mL ampicillin and 34μg/mL chloramphenicol. Cells were cultured at 37°C until OD_{595} was equal to 0.8. Protein expression was induced by addition of 0.1mM IPTG and cultured for an additional 16 – 18 hours at 25 °C. Cells were harvested by centrifugation (5000 rpm for 30 min) and the periplasmic *E. coli* fraction was extracted via osmotic shock as described [30]. Briefly,

harvested cells were suspended in a hypertonic solution of 30mM Tris, 20% w/v sucrose, 1mM EDTA, pH 8.0 (25mL / 1L culture) and incubated for 30 min at 4°C. Then, cells were centrifuged at 20.000 x g at 4°C for 20 min and the supernatant was collected (sup1). Cells were re-suspended in a hypotonic solution of 5mM $MgSO_4$ (25 ml / 1L culture), incubated for 30 min at 4°C and followed by an additional centrifugation at 20000 x g at 4°C for 20 min (sup2). The supernatant (sup2) from the hypotonic solution was used for the purification step.

The periplasmic solution containing secreted *SAP2* was purified by Ni^{2+} affinity chromatography as follows. A 6.5mL Ni-NTA agarose column was equilibrated with 20mM Tris, 300mM NaCl, 40mM imidazole, pH 8.0. The clarified osmotic shock fluid (sup2) was loaded onto the column and washed with equilibration buffer for 15 column volumes (CV). Bound protein was eluted with 5 CVs of 20mM Tris, 300mM NaCl, 500mM imidazole, pH 8.0. Fractions with an absorbance at 59 nm (Bradford assay) greater than 0.5 were pooled, concentrated and buffer exchanged into 50mM Tris-HCl pH 8.0, 25mM NaCl, 10% glycerol with dialysis membrane (6-8kDa MWCO) overnight at 4°C.

1-NPN binding competition assays

The affinity of various insecticides for *SAP1*, *SAP2* and *SAP3* was measured indirectly by competitive binding assays, which determined the displacement of the ligands from the SAPs by the fluorescent probe N-phenyl-1-naphthylamine (1-NPN). Purified recombinant SAP proteins were mixed with different concentrations of insecticides (in methanol) and 1-NPN (in methanol) in a final volume of 200µl 20 mM Tris-HCl, pH 8.0, 100mM NaCl (containing 1.5% methanol). The final concentration of recombinant SAP protein and 1-NPN in the assays was 10µM and 5µM respectively. Insecticide concentration ranged from 0.0625-20µM. The probe was excited at 337 nm and emission spectra were recorded between 380nm and 460nm (peak emission in the presence of recombinant SAP is at 386-388nm). Emission spectra were recorded on an Infinite M-200 fluorimeter (Tecan Trading AG, Switzerland) using black 96 well plates (Greiner Bio-One, Austria). Graphs were produced using GraphPad Prism 8.0.2 (La Jolla California USA, www.graphpad.com). A non-linear fit using logged concentrations were used to fit best fit lines and calculate the IC50s. The calculated log IC50s and associated standard errors were used to fit an ANOVA to compare the binding specificity of the 3 proteins.

Microarray Data

Microarray data was retrieved from the IR-TEx Application [10] (https://www.lstmed.ac.uk/projects/ir-tex).

Field Collections

Field collections of *An. gambiae* s. l. were performed by LSTM colleagues in collaboration with the Centre National de Recherche sur le Paludsime (CNRFP) in Banfora district, Burkina Faso. The mosquitoes used in this study originated from Tengrela, (10°38’7.53”N; 4°48’48.35”W) in 2011, 2012, 2014, 2016 and 2018, Bakaridjan (10°24’26.34”N; 4°33’44.78”W) in 2013 and 2015 and from Tiefora (10°37’54.02”N; 4°33’22.85”W) in

2018. All gDNA extractions were subject to SINE PCR [31] to determine the species of each mosquito before sequencing.

Scan for natural selection

We computed iHS [20] and XPEHH [21] statistics on phased sequences for regions 1.5Mbp upstream and downstream of the chemosensory locus for all available *An. gambiae* West African mosquito populations found in phase 2 of the *Anopheles* 1000 Genomes project using scikit-allel v1.1.10 (DOI: 10.5281/zenodo.822784). A peak was apparent in iHS in the Guinean *A. gambiae* population (highest value at 3R: 4,845,138), and a smaller peak was present in Burkina Faso, a XPEHH peak was present in Cameroon.

Clustering analysis and SNP Panel

We carried out haplotype clustering analysis around the chemosensory locus and identified 13 haplotypes that differed by fewer than 20 SNPs across a window 25kb up and downstream of the limits of *SAP2*. This is a firm proxy for identity by descent in an organism with pi ~ 0.01 [19], indicative of selection acting at this region. These 13 shared haplotypes were observed in Guinea, Burkina Faso and Cameroon.

These 13 haplotypes were used to define 55 SNPs showing high Fst between this cluster and the wild type *An. gambiae* populations. A SNP panel screen was designed to encompass a range of these SNPs showing the highest delta between wild type and cluster SNPs, primers for the two panels were as follows:: -F: CAAGCATTGCGCCATCGT; -R: GAGAAGATGATACTGAGCGG. PCR was performed on gDNA from individual *An. gambiae* from Bakaridjan in 2013 (42 individuals) and 2015 (50 individuals) and Tiefora in 2018 (40 individuals). SNP genotypes from genomic sequence data from individual *An. coluzzii* samples from Tengrela from 2011 (21 individuals), 2012, 2014 and 2016 (72 individuals for each year) was kindly provided by the Broad Institute; the PCR panel was ran on samples from the same site in 2018 (20 samples). The panel was ran using Phusion High-Fidelity DNA Polymerase (Thermo Fisher, UK) following manufacturer's instructions and the cycles: 98°C for 30 seconds, 35 cycles of: 98°C for 7 seconds, 65°C for 10s, 72°C for 15 seconds and a final 72°C, 15-minute hold. The resultant product was purified using a QiaQuick Gel Extraction Kit (Qiagen, UK) following manufacturer's instructions and sent for Sanger sequencing at Eurofins Genomics, UK using the reverse primer. SNPs were identified using Benchling [Biology Software] (2019, https://benchling.com) and the resultant change in minor allele frequency calculated and a trendline fitted to each SNP using GraphPad Prism 8.0.2 (La Jolla California USA, www.graphpad.com).

Phylogeny

cDNA sequences for each of the CSPs were retrieved from VectorBase [32] and aligned using Clustal Omega (https://www.ebi.ac.uk/Tools/msa/clustalo/). These data were loaded into Mega 7.0 [33] and a maximum likelihood tree with 1000 bootstraps performed.

Extended Data

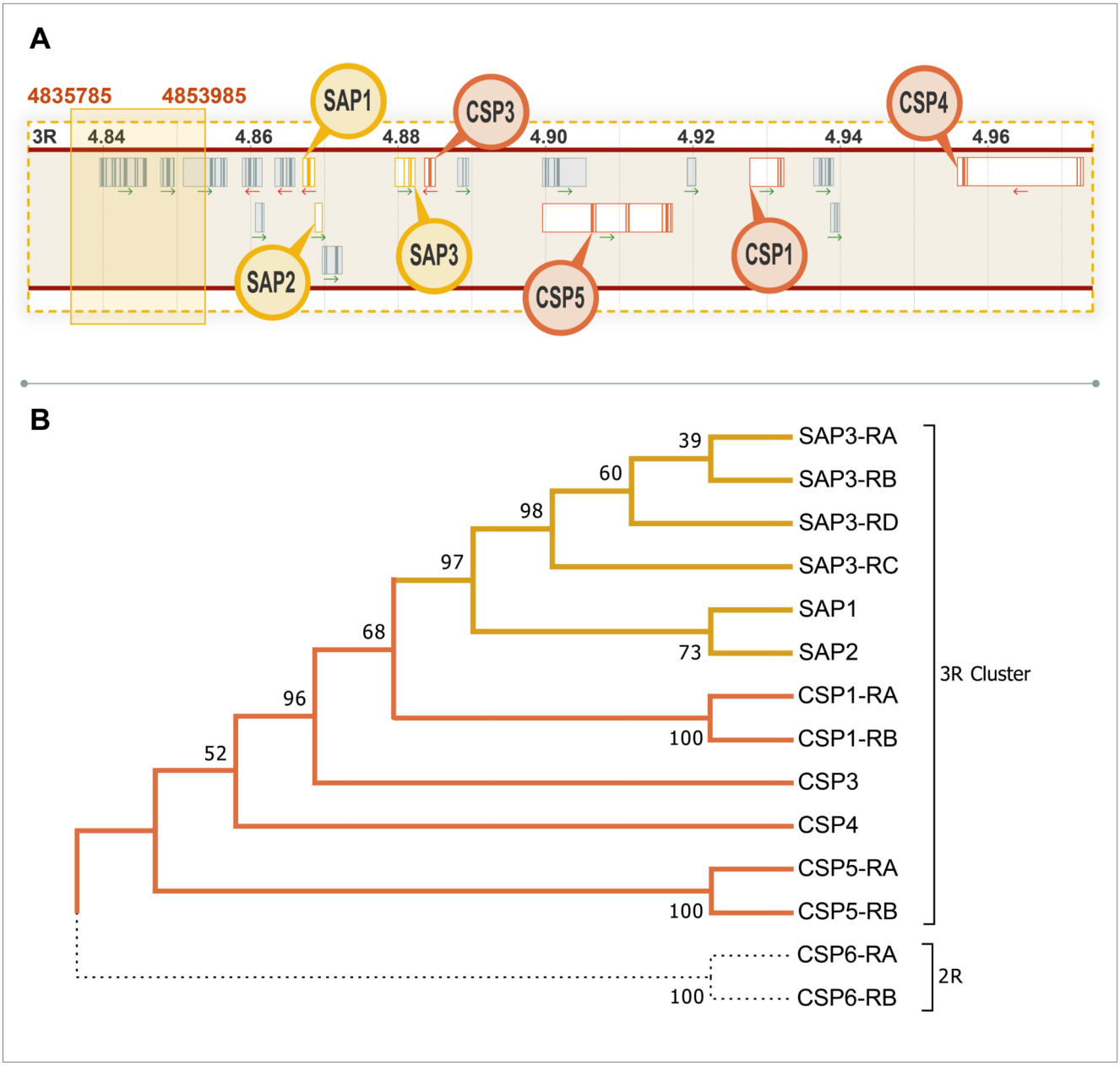

Extended Data Figure 1. Chemosensory protein cluster.

A. Schematic of the region surrounding the shared haplotype block found in the 1000 genomes data with all chemosensory proteins in the cluster highlighted in yellow. Genes displayed in order of appearance, left to right, are as follows: AGAP008046, AGAP013713, AGAP008047, AGAP008048, AGAP008049, AGAP008050, AGAP008051 (*SAP1*), AGAP008052 (*SAP2*), AGAP008053, AGAP008054 (*SAP3*), AGAP008055 (*CSP3*), AGAP008056, AGAP029127 (*CSP5,* previously AGAP008058), AGAP008059 (*CSP1*), AGAP008060, AGAP008061 and AGAP008062 (*CSP4*). **B.** cDNA bootstrap consensus tree inferred from 1000 replicates using the maximum likelihood method; the percentage of replicate trees with the associated clustering are shown next to the branches. Yellow

indicates the sensory appendage proteins, orange the remaining chemosensory proteins in the 3R cluster and black dotted lines show *CSP6*, which is located on 2R. Alternative isoforms are represented with -RX, with X proceeding alphabetically dependent on number of splice variants.

Europe PMC Funders Author Manuscripts

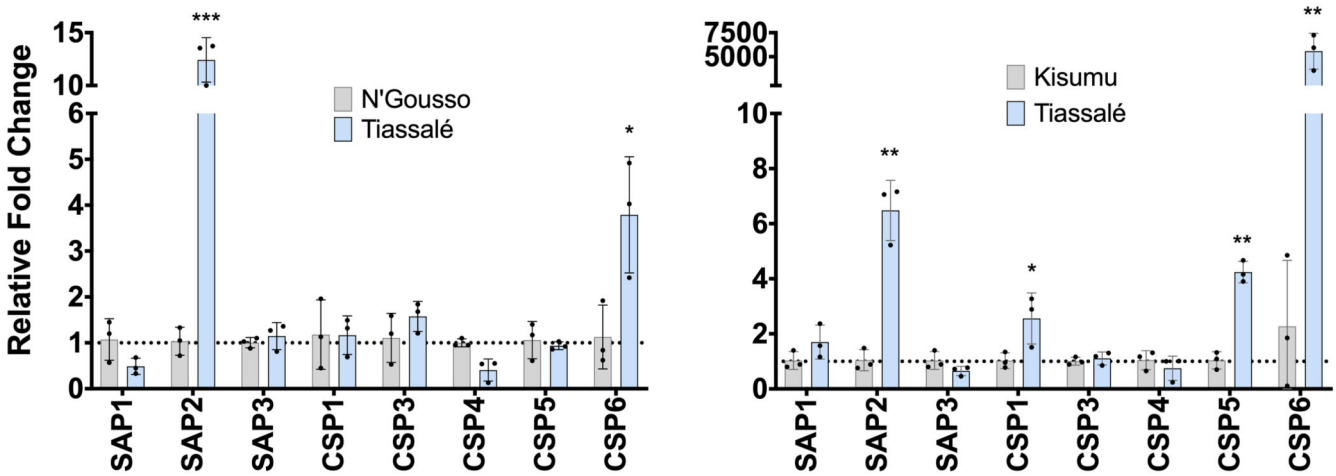

Extended Data Figure 2. Overexpression of CSP family in a multi-resistant *Anopheles* population.

The left panel shows mean relative fold change of each CSP in Tiassalé mosquitoes (blue) compared to the susceptible control N'Gousso (grey) as determined by qPCR, the right panel compared to the susceptible population Kisumu (grey). Points show 3 biological replicates and error bars show standard deviation. * $p \leq 0.05$; ** $p \leq 0.01$; *** $p \leq 0.001$. Statistical significance calculated by an ANOVA followed by Dunnett's *post hoc* test; p-values are in Supplementary Table 2.

Europe PMC Funders Author Manuscripts

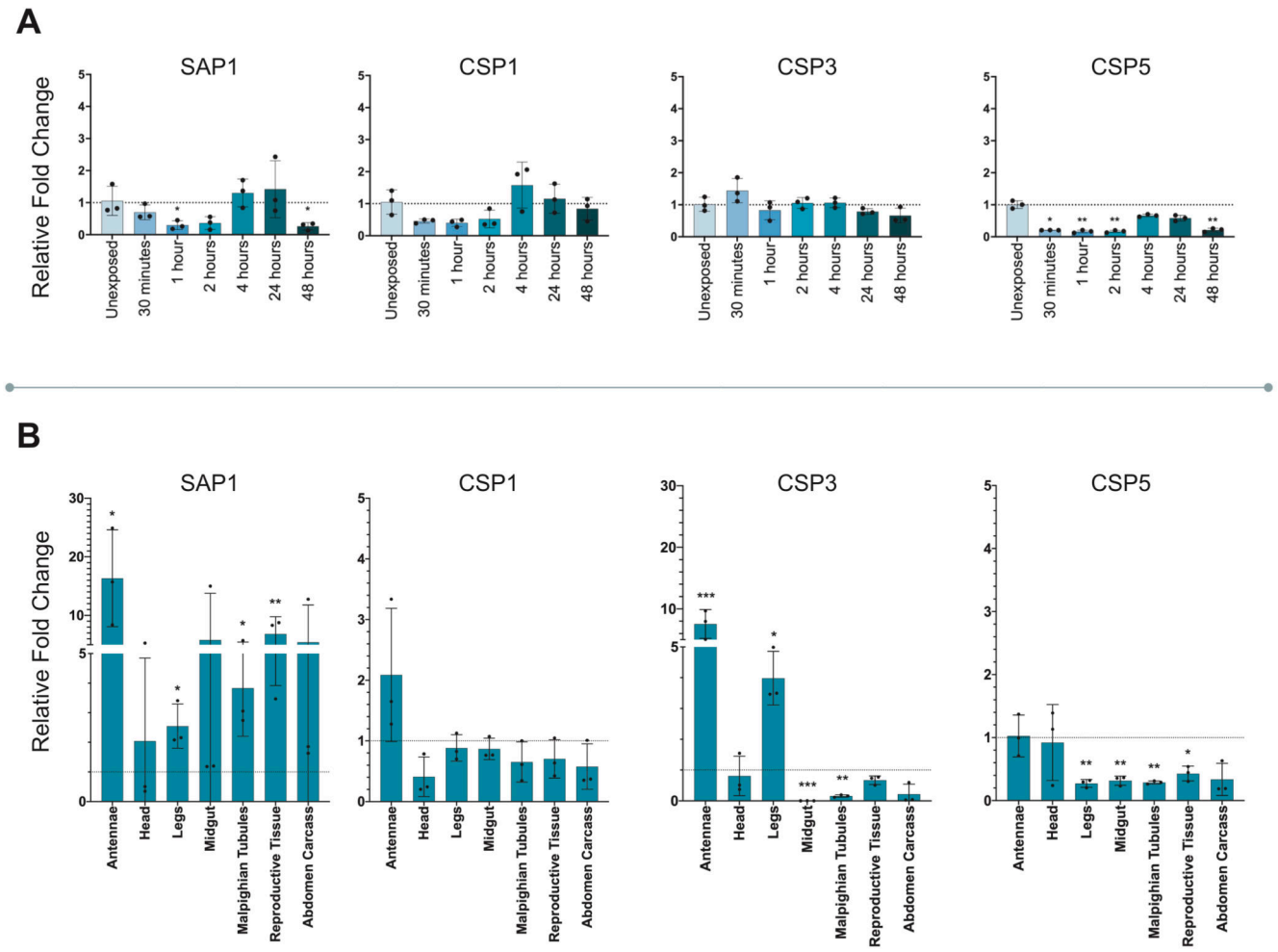

Extended Data Figure 3. Expression levels of non-induced chemosensory proteins post-deltamethrin exposure in Tiassalé.

A. Expression levels of the remaining four CSPs at various time points post-deltamethrin exposure in the multi-resistant population Tiassalé. **B.** Tissue specific induction of these four CSPs 4-hours post-deltamethrin exposure. The data show mean of 3 biological replicates ± standard deviation. * $p \leq 0.05$; ** $p \leq 0.01$; *** $p \leq 0.001$. Statistical significance calculated by an ANOVA followed by Dunnett's *post hoc* test. If the data was non-normal, data was analysed using Kruskall-Wallis followed by a Dunn's *post hoc* test; p-values are in Supplementary Table 2.

Europe PMC Funders Author Manuscripts

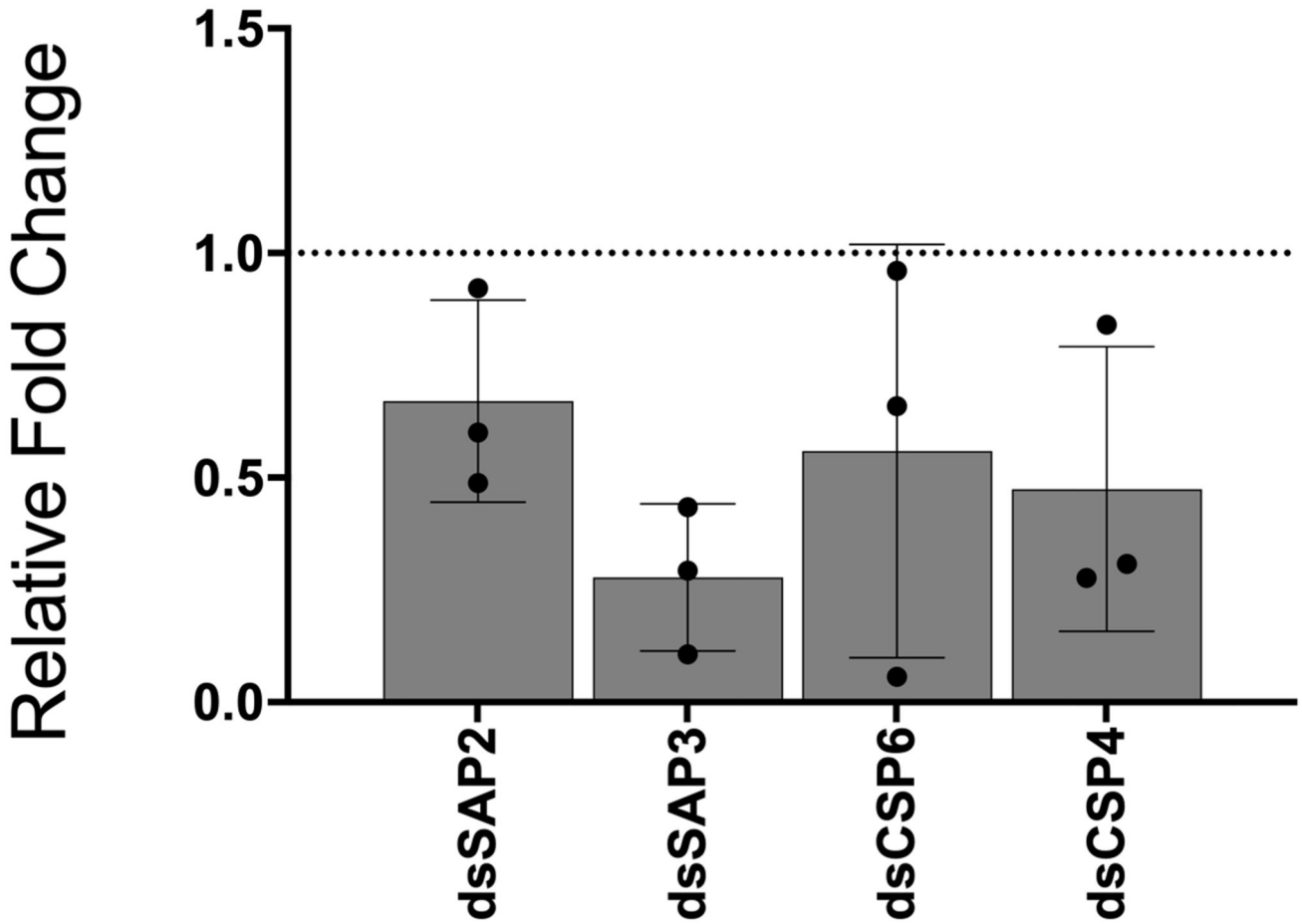

Extended Data Figure 4. Efficacy of RNAi.

mRNA knockdown of whole female mosquitoes 72-hours post injection compared to GFP injected controls. Mean of 3 biological replicates and standard deviation shown.

Europe PMC Funders Author Manuscripts

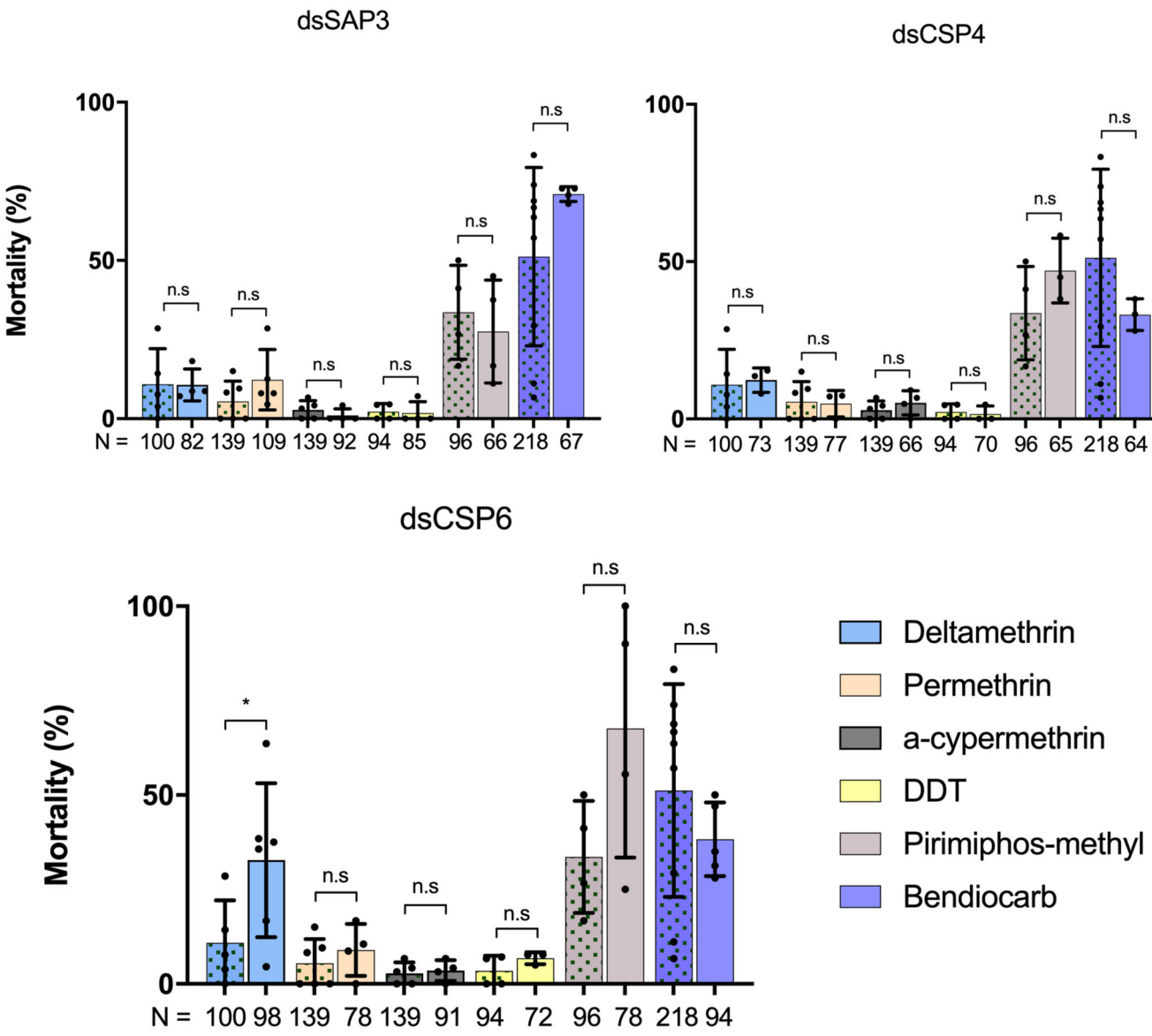

Extended Data Figure 5. Phenotype of other induced CSPs to a panel of insecticides.

Effect of attenuation of (a) ds*SAP3* ($n_{deltamethrin}$ = 4; $n_{permethrin}$ = 5; $n_{\alpha\text{-cypermethrin}}$ = 3; n_{DDT} = 3; $n_{pirimiphos\text{-}methyl}$ = 3; $n_{bendiocarb}$ = 4) (b) ds*CSP4* ($n_{deltamethrin}$ = 3; $n_{permethrin}$ = 3; $n_{\alpha\text{-cypermethrin}}$ = 3; n_{DDT} = 3; $n_{pirimiphos\text{-}methyl}$ = 3; $n_{bendiocarb}$ = 3) and (c) *dsCSP6* ($n_{deltamethrin}$ = 6; $n_{permethrin}$ = 4; $n_{\alpha\text{-cypermethrin}}$ = 4; n_{DDT} = 3; $n_{pirimiphos\text{-}methyl}$ = 4; $n_{bendiocarb}$ = 5) on mortality after insecticide exposure in Tiassalé mosquitoes (right bars) compared to dsGFP injected controls (left bars, green patterned; $n_{deltamethrin}$ = 5; $n_{permethrin}$ = 5; $n_{\alpha\text{-cypermethrin}}$ = 5; n_{DDT} = 4; $n_{pirimiphos\text{-}methyl}$ = 4; $n_{bendiocarb}$ = 8). Analysis of mortality data was done using an ANOVA test followed by a Tukey *post hoc* test, n.s indicates a non-significant change in mortality, * $p \leq 0.05$. ds*CSP6* $\mu_{mortality}$ = 11.7% to 31.6%, p = 0.0474. N shows number of individual mosquitoes used for phenotyping; points show the number of bioassay replicates per group. Error bars show standard deviation.

Europe PMC Funders Author Manuscripts

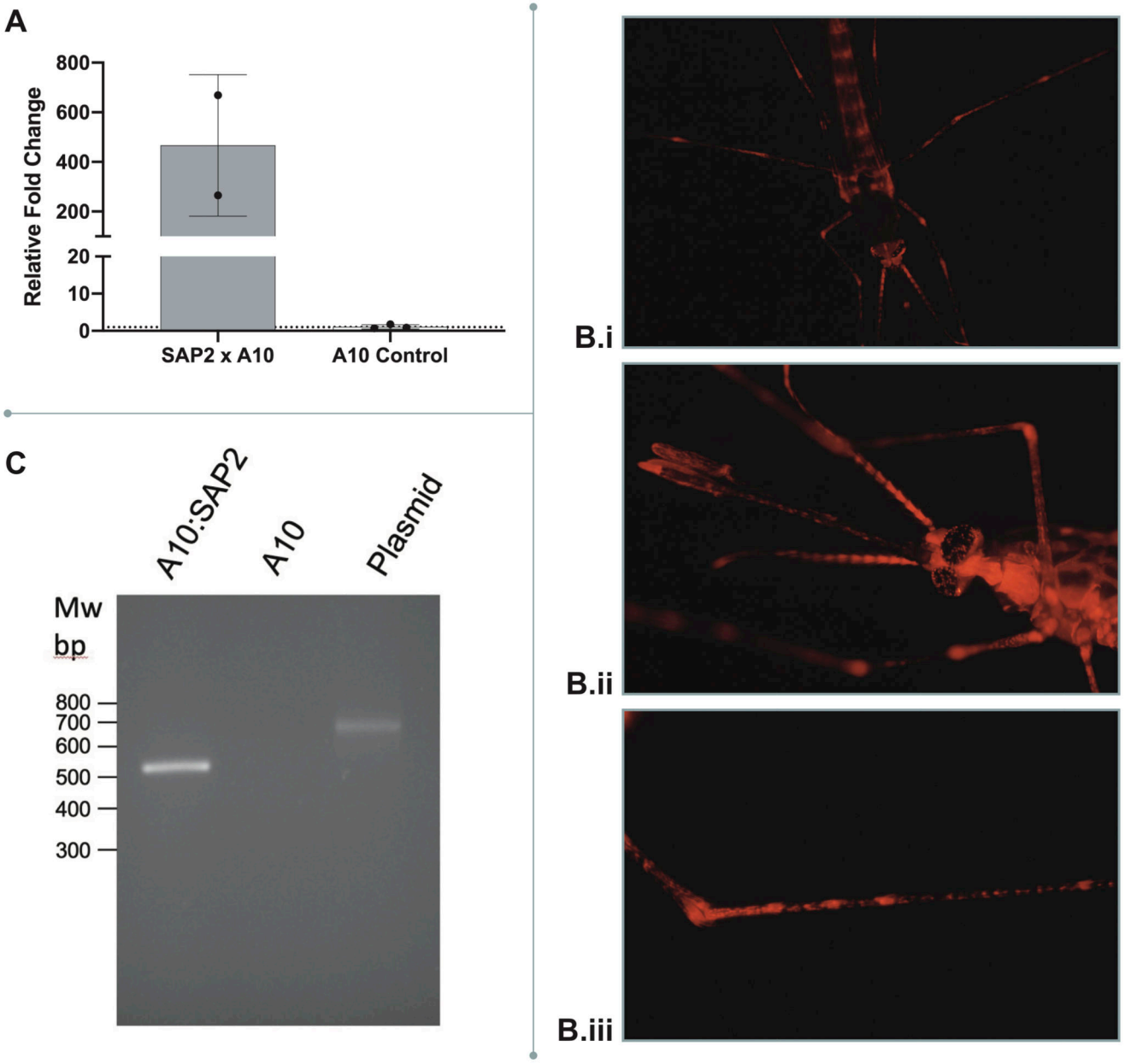

Extended Data Figure 6. Characterisation of *SAP2* in the transgenic line.

A. Mean mRNA expression of *SAP2* overexpression in the *SAP2* x A10 transgenic line (n=2) compared to *SAP2* in the A10 x G3 control (n = 3). Error bars represent standard deviation and points show each biological replicate. **B.** mCherry under the *Polyubiquitin c* A10 promoter demonstrating (i) ubiquitous expression; (ii) expression in the head; (iii) expression in the legs as shown previously by Adolfi et al. 2018; these results were tested across over a hundred independent mosquito screenings. **C.** Intron splicing confirmed by PCR in A10 x *SAP2* and negative control A10 mosquitoes compared to plasmid DNA: pUAS-*SAP2*. Size of PCR product with and without synthetic intron 647bp and 534bp,

respectively. MW: 100bp DNA ladder. 2 samples A10 x *SAP2* and 2 control samples A10 (each sample: pool of 5 females, 4 days old, unfed) were tested and repeated in two PCRs.

Europe PMC Funders Author Manuscripts

Europe PMC Funders Author Manuscripts

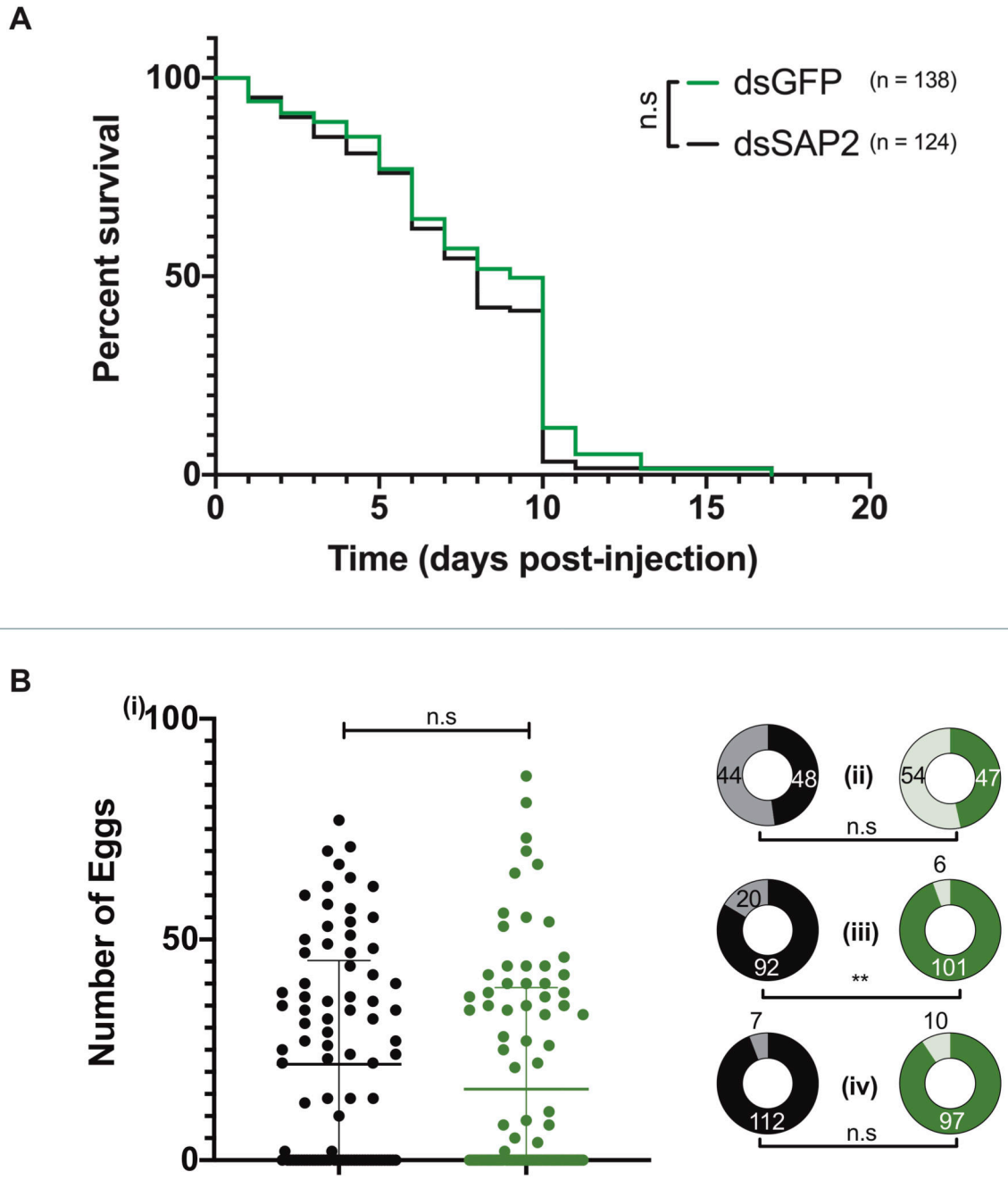

Extended Data Figure 7. Effect of dsSAP2 injection on Tiassalé fitness.

A. Longevity of dsSAP2 (black) compared to dsGFP controls (green). N shows number of individual mosquitoes used in each group; n.s represents p = 0.113 as calculated by a Mantel-Cox test (two-sided). **B.** Life history traits in dsSAP2 injected (black) and dsGFP injected (green) females (i) Number of eggs in each group 72-hours post-blood meal, median and interquartile range displayed; (ii) Proportion of females with eggs (Dark shading are females with eggs, light without; p = 0.4382); (iii) Mortality post-blood meal (Dark shading are females alive post-blood meal, light those dead; p = 0.0052); (iv) Blood feeding

proportions (Dark shading are blood fed females, light non-blood fed; $p = 0.3257$); for dsSAP2 injected and dsGFP injected controls (green). Numbers show total individual females in each group. Significance in (i) as calculated by a two tailed Mann-Whitney U test (n.s represents $p = 0.0657$); (ii), (iii) and (iv) through a chi-squared test. ** $p \leq 0.01$.

Europe PMC Funders Author Manuscripts

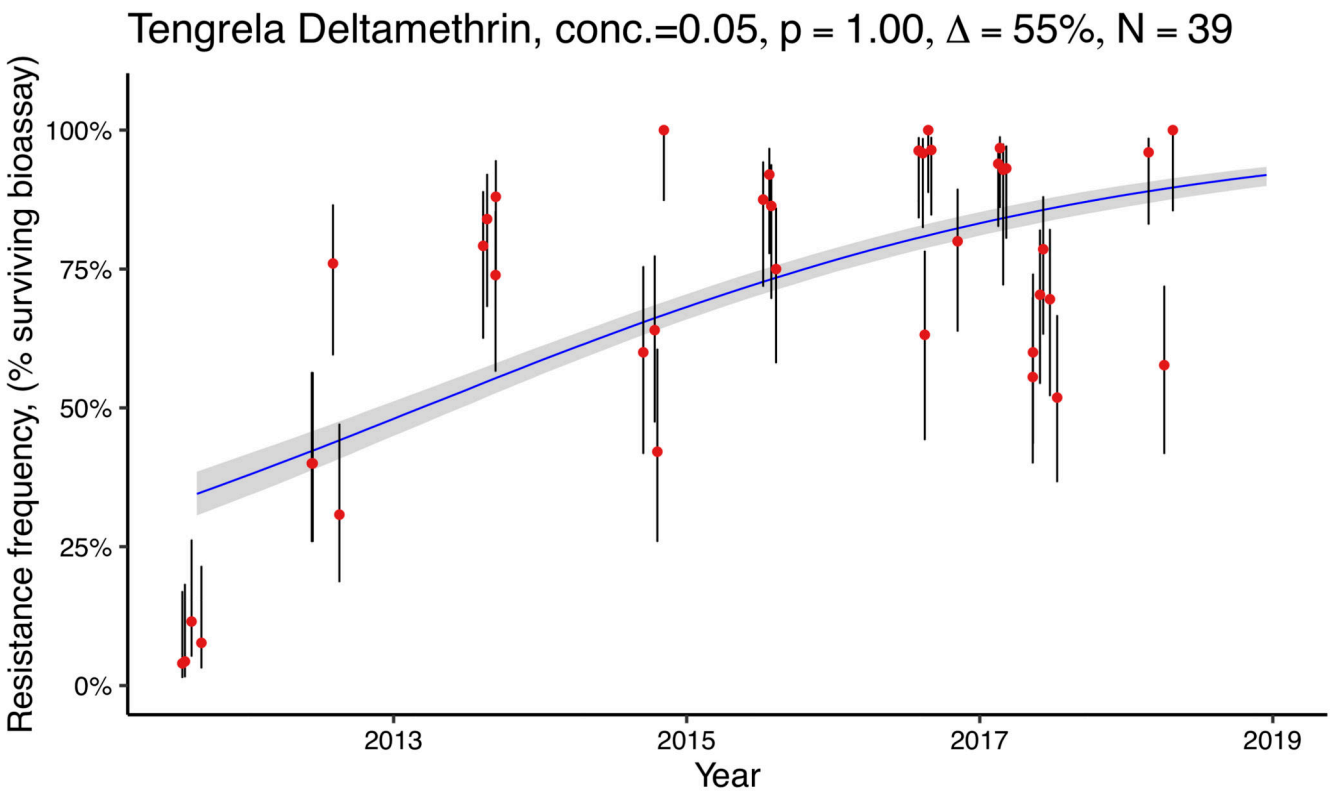

Extended Data Figure 8. Mortality of *An. coluzzii* field populations.

Temporal plot of mortality from 2011 to 2018 of *An. coluzzii* mosquitoes to 0.05% WHO tube deltamethrin exposure, Δ is the posterior median change in mortality from 2011 to 2018, N is number of experiments included (minimum sample size for any given data point = 14), P the posterior probability that resistance (the proportion of posterior samples where the April 2018 mean exceeds the corresponding value in January 2011) has increased over the time period. The blue line indicates the posterior median of a logistic model fit to binomial test results; the two parameters of the logistic function were assigned uninformative (Cauchy(0, 1)) priors. The model was fit using Stan[23] using 4 chains and 800 iterations per chain (400 of which were discarded as warm-up in each case); all parameters had Rhat < 1.1 indicating convergence. The shading indicates the 90% predictive interval on the mean. Data and Figure kindly provided by Dr Hyacinthe Toé, Dr Ben Lambert and Dr Thomas Churcher.

Extended Data Figure 9. Sequencing of SAP2 primer binding sites.

4 N'Gousso individuals and 4 Tiassale individuals were sequenced across the primer binding sites. (a) Complete conservation of sequence was seen in the forward binding site (b) one N'Gousso individual was heterozygous at one base in the centre of the reverse primer binding site.

Europe PMC Funders Author Manuscripts

Extended Data Table 1

Expression of CSP family in Western Africa.

Microarray fold change data from microarray datasets retrieved from IR-TEx[10] across Western Africa for *An. coluzzii* and *An. gambiae* populations for each member of the CSP family. Highlighted in green are fold changes showing significant overexpression in the respective datasets, and yellow under expression; white backgrounds show no significant change. *SAP2* is emboldened. The country of origin, species and exposure status of the resistant population are given below each table, as well as the susceptible population used as a comparator.

Dataset		**Banfora**	**Tiefora13**	**Tiefora14**	**Tensrela**	**VK72011**	**VK72012**	**VK6**
AGAP008051-RA	SAP1	0.827	3.320	5.414	2.229	2.006	0.370	0.402
AGAP008052-RA	**SAP2**	**2.218**	**2.947**	**7.912**	**6.102**	**6.322**	**0.953**	**0.949**
AGAP008054-RA	SAP3	1.040	0.882	0.736	1.052	1.729	0.858	1.329
AGAP008055-RA	CSP3	0.960	2.516	1.994	3.086	3.866	0.914	1.419
AGAP008058-RA	CSP5	1.060	1.252	1.824	1.074	1.231	0.649	0.997
AGAP008059-RA	CSP1	0.506	3.628	4.146	1.738	1.247	0.466	0.877
AGAP008062-RA	CSP4	0.921	0.992	1.024	0.948	1.048	0.985	1.162
AGAP001303-RA	CSP6	0.869	1.772	2.118	0.961	0.704	0.463	0.782
AGAP001303-RB	CSP6	0.864	1.821	2.164	0.969	0.711	0.444	1.195
Country		**Burkina Faso**	**Burkina Faso**	**Burkina Faso**	**Burkina Faso**	**Burkina Faso**	**Burkina Faso**	**Burkina Faso**
Species		**An. coluzzii**	**An. gambiae**	**An. gambiae**	**An. coluzzii**	**An. coluzzii**	**An. coluzzii**	**An. coluzzii**
Exposure Status		Unexposed	Unexposed	Unexposed	Unexposed	Deltamethrin	Deltamethrin	Unexposed
Susceptible Comparator		N'Gousso	Kisumu	Kisumu	Mali	Mali	N'Gousso	N'Gousso
Dataset		**Bouake**	**M'Be**	**Tiassale**	**TiassaleMali**	**TiassaleOkyero**	**Tiassale2011**	**Nkolondom**
AGAP008051-RA	SAP1	1.889	1.726	4.257	1.106	0.620	0.385	1.374
AGAP008052-RA	**SAP2**	**10.486**	**8.882**	**51.346**	**1.360**	**0.419**	**0.768**	**1.415**
AGAP008054-RA	SAP3	2.585	1.683	5.516	0.822	0.623	0.681	1.844
AGAP008055-RA	CSP3	1.157	1.549	1.247	1.091	0.672	0.569	2.259
AGAP008058-RA	CSP5	0.946	1.134	1.008	1.038	0.833	0.688	1.330
AGAP008059-RA	CSP1	1.609	1.932	2.505	1.067	0.844	0.638	1.331
AGAP008062-RA	CSP4	0.992	0.980	0.995	1.076	0.990	1.128	1.100
AGAP001303-RA	CSP6	0.610	0.635	0.856	0.848	1.130	0.456	2.384
AGAP001303-RB	CSP6	0.584	0.604	0.819	0.850	1.065	0.458	2.463

Country		Cote D'Ivoire	Cote D'Ivoire	Cote D'Ivoire	Cote D'Ivoire	Cote D'Ivoire	Cote D'Ivoire	Cameroon
Species		**An. coluzzii**	**An. coluzzii**	**An. coluzzii**	**An. coluzzii**	**An. coluzzii**	**An. coluzzii**	**An. gambiae**
Exposure Status		Deltamethrin	Deltamethrin	Deltamethrin	Unexposed	Unexposed	Unexposed	DDT
Susceptible Comparator		N'gousso	N'gousso	N'gousso	Mali	Okyero	N'Gousso	Kisumu
Dataset		**Garre**	**Messa**	**Youande**	**Bioko**	**KovieOkyero**	**KovieMalanville**	
AGAP008051-RA	SAP1	0.659	0.702	0.978	0.782	1.171	0.519	
AGAP008052-RA	**SAP2**	**3.024**	**1.673**	**2.009**	**4.094**	**0.871**	**0.473**	
AGAP008054-RA	SAP3	1.480	1.842	1.412	0.962	0.605	0.065	
AGAP008055-RA	CSP3	1.023	0.795	0.952	0.754	0.723	0.844	
AGAP008058-RA	CSP5	0.774	0.681	1.298	0.734	0.842	0.956	
AGAP008059-RA	CSP1	0.481	0.492	1.297	0.472	1.535	1.293	
AGAP008062-RA	CSP4	0.958	0.870	0.993	0.848	1.821	0.826	
AGAP001303-RA	CSP6	0.452	0.423	1.387	0.458	1.135	0.896	
AGAP001303-RB	CSP6	0.450	0.393	1.431	0.435	1.232	0.908	

Country		Cameroon	Cameroon	Cameroon	Equatorial Guinea	Togo	Togo
Species		**An. coluzzii**	**An. coluzzii**	**An. gambiae**	**An. coluzzii**	**An. coluzzii**	**An. coluzzii**
Exposure Status		DDT	DDT	Bendiocarb	Deltamethrin	Unexposed	Unexposed
Susceptible Comparator		N'Gousso	N'Gousso	N'Gousso	N'gousso	Okyero	Malanville

Supplementary Material

Refer to Web version on PubMed Central for supplementary material.

Europe PMC Funders Author Manuscripts

Acknowledgements

Thank you to the following for providing field collections: Dr Nelson Grisales, LSTM (Bakaridjan in 2013 and 2015); Dr Antoine Sanou, Dr Moussa Guelbeogo, CNRFP (Tiefora 2018, Tengrela 2011, 2012, 2014, 2016); Natalie Lissenden, LSTM (Tengrela 2018). We are grateful to Dr Daniel Neafsey and Dr Jacob Tennessen, Broad Institute for sharing Tengrela whole genome sequence data, Dr Immacolata Iovinella, University of Florence for provision of *SAP1* and *SAP3* plasmids, Manuela Bernardi, LSTM for help with figure preparation and to Faye Brown, Sara Elg, Patricia Pignatelli and Derek Au, LSTM for providing some technical support. We are also grateful to Dr Hyacinthe Toé and Dr Thomas Churcher for supplying both the field data and figure in Extended Data Figure 8. We finally thank Dimitra Tsakireli (IMBB-FORTH) and Evangelia Morou (IMBB-FORTH), for their help for the expression and characterisation of SAP proteins.

Funding

This study was funded by an MRC Skills Development Fellowship (MR/R024839/1) to V.I and a Royal Society Challenge Grant (CH160059) to H.R. Mosquito collections in Burkina Faso were supported by EC FP7 Project grant no: 265660 “AvecNet” and Wellcome Trust Collaborative Award (200222/Z/15/Z).

References

1. Bhatt S, et al. The effect of malaria control on Plasmodium falciparum in Africa between 2000 and 2015. Nature. 2015; 526:207–211. [PubMed: 26375008]
2. WHO. World Malaria Report. Geneva: 2018.
3. Hawley WA, et al. Community-wide effects of permethrin-treated bed nets on child mortality and malaria morbidity in western Kenya. Am J Trop Med Hyg. 2003; 68:121–127. [PubMed: 12749495]
4. Churcher TS, Lissenden N, Griffin JT, Worrall E, Ranson H. The impact of pyrethroid resistance on the efficacy and effectiveness of bednets for malaria control in Africa. Elife. 2016; 5:e16090. [PubMed: 27547988]
5. Protopopoff N, et al. Effectiveness of a long-lasting piperonyl butoxide-treated insecticidal net and indoor residual spray interventions, separately and together, against malaria transmitted by pyrethroid-resistant mosquitoes: a cluster, randomised controlled, two-by-two fact. Lancet. 2018; 391:1577–1588. [PubMed: 29655496]
6. Stevenson BJ, et al. Cytochrome P450 6M2 from the malaria vector Anopheles gambiae metabolizes pyrethroids: Sequential metabolism of deltamethrin revealed. Insect Biochem Mol Biol. 2011; 41:492–502. [PubMed: 21324359]
7. Müller P, et al. Field-Caught Permethrin-Resistant Anopheles gambiae Overexpress CYP6P3, a P450 That Metabolises Pyrethroids. PLoS Genet. 2008; 4:e1000286. [PubMed: 19043575]
8. Gleave K, Lissenden N, Richardson M, Ranson H. Piperonyl butoxide (PBO) combined with pyrethroids in long-lasting insecticidal nets (LLINs) to prevent malaria in Africa. Cochrane Database Syst Rev. 2017
9. Toe KH, et al. Do bednets including piperonyl butoxide offer additional protection against populations of Anopheles gambiae sl. that are highly resistant to pyrethroids? An experimental hut evaluation in Burkina Fasov. Med Vet Entomol. 2018
10. Ingham VA, Wagstaff S, Ranson H. Transcriptomic meta-signatures identified in Anopheles gambiae populations reveal previously undetected insecticide resistance mechanisms. Nat Commun. 2018; 9
11. Edi CV, et al. CYP6 P450 Enzymes and ACE-1 Duplication Produce Extreme and Multiple Insecticide Resistance in the Malaria Mosquito Anopheles gambiae. PLoS Genet. 2014; 10:e1004236. [PubMed: 24651294]
12. Vieira FG, Rozas J. Comparative genomics of the odorant-binding and chemosensory protein gene families across the Arthropoda: origin and evolutionary history of the chemosensory system. Genome Biol Evol. 2011; 3:476–90. [PubMed: 21527792]
13. Leal WS. Odorant reception in insects: roles of receptors, binding proteins, and degrading enzymes. Annu Rev Entomol. 2013; 58:373–391. [PubMed: 23020622]
14. Iovinella I, Bozza F, Caputo B, della Torre A, Pelosi P. Ligand-binding study of Anopheles gambiae chemosensory proteins. Chem Senses. 2013; 38:409–419. [PubMed: 23599217]

15. Xuan N, et al. Increased expression of CSP and CYP genes in adult silkworm females exposed to avermectins. Insect Sci. 2015; 22:203–219. [PubMed: 24677614]
16. Bautista MAM, et al. Evidence for trade-offs in detoxification and chemosensation gene signatures in Plutella xylostella. Pest Manag Sci. 2015; 71:423–432. [PubMed: 24796243]
17. Liu GX, et al. Biotype expression and insecticide response of Bemisia tabaci chemosensory protein-1. Arch Insect Biochem Physiol. 2014; 85:137–151. [PubMed: 24478049]
18. Yunta C, et al. Pyriproxyfen is metabolized by P450s associated with pyrethroid resistance in An. gambiae. Insect Biochem Mol Biol. 2016; 78:50–57. [PubMed: 27613592]
19. Consortium, A. gambiae 1000 G. Genetic diversity of the African malaria vector Anopheles gambiae. Nature. 2017; 552:96. [PubMed: 29186111]
20. Voight BF, Kudaravalli S, Wen X, Pritchard JK. A Map of Recent Positive Selection in the Human Genome. PLOS Biol. 2006; 4:e72. [PubMed: 16494531]
21. Sabeti PC, et al. Genome-wide detection and characterization of positive selection in human populations. Nature. 2007; 449:913. [PubMed: 17943131]
22. Pombi M, et al. Unexpectedly high Plasmodium sporozoite rate associated with low human blood index in Anopheles coluzzii from a LLIN-protected village in Burkina Faso. Sci Rep. 2018; 8
23. Carpenter B, et al. Stan: A probabilistic programming language. J Stat Softw. 2017; 76
24. Namountougou M, et al. Multiple insecticide resistance in Anopheles gambiae sl populations from Burkina Faso, West Africa. PLoS One. 2012; 7:e48412. [PubMed: 23189131]
25. Harris C, et al. Polymorphisms in Anopheles gambiae immune genes associated with natural resistance to Plasmodium falciparum. PLoS Pathog. 2010; 6:e1001112. [PubMed: 20862317]
26. Adolfi A, Pondeville E, Lynd A, Bourgouin C, Lycett GJ. Multi-tissue GAL4-mediated gene expression in all Anopheles gambiae life stages using an endogenous polyubiquitin promoter. Insect Biochem Mol Biol. 2018; 96:1–9. [PubMed: 29578046]
27. Organization, W. H.. Test procedures for insecticide resistance monitoring in malaria vector mosquitoes. 2016.
28. Severo MS, et al. Unbiased classification of mosquito blood cells by single-cell genomics and high-content imaging. Proc Natl Acad Sci. 2018; 115:E7568–E7577. [PubMed: 30038005]
29. Schmittgen TD, Livak KJ. Analyzing real-time PCR data by the comparative CT method. Nat Protoc. 2008; 3:1101–1108. [PubMed: 18546601]
30. Sockolosky JT, Szoka FC. Periplasmic production via the pET expression system of soluble, bioactive human growth hormone. Protein Expr Purif. 2013; 87:129–135. [PubMed: 23168094]
31. Santolamazza F, et al. Insertion polymorphisms of SINE200 retrotransposons within speciation islands of Anopheles gambiae molecular forms. Malar J. 2008; 7:163. [PubMed: 18724871]
32. Giraldo-Calderón GI, et al. VectorBase: an updated bioinformatics resource for invertebrate vectors and other organisms related with human diseases. Nucleic Acids Res. 2014; 43:D707–D713. [PubMed: 25510499]
33. Kumar S, Stecher G, Tamura K. MEGA7: molecular evolutionary genetics analysis version 7.0 for bigger datasets. Mol Biol Evol. 2016; 33:1870–1874. [PubMed: 27004904]

Europe PMC Funders Author Manuscripts

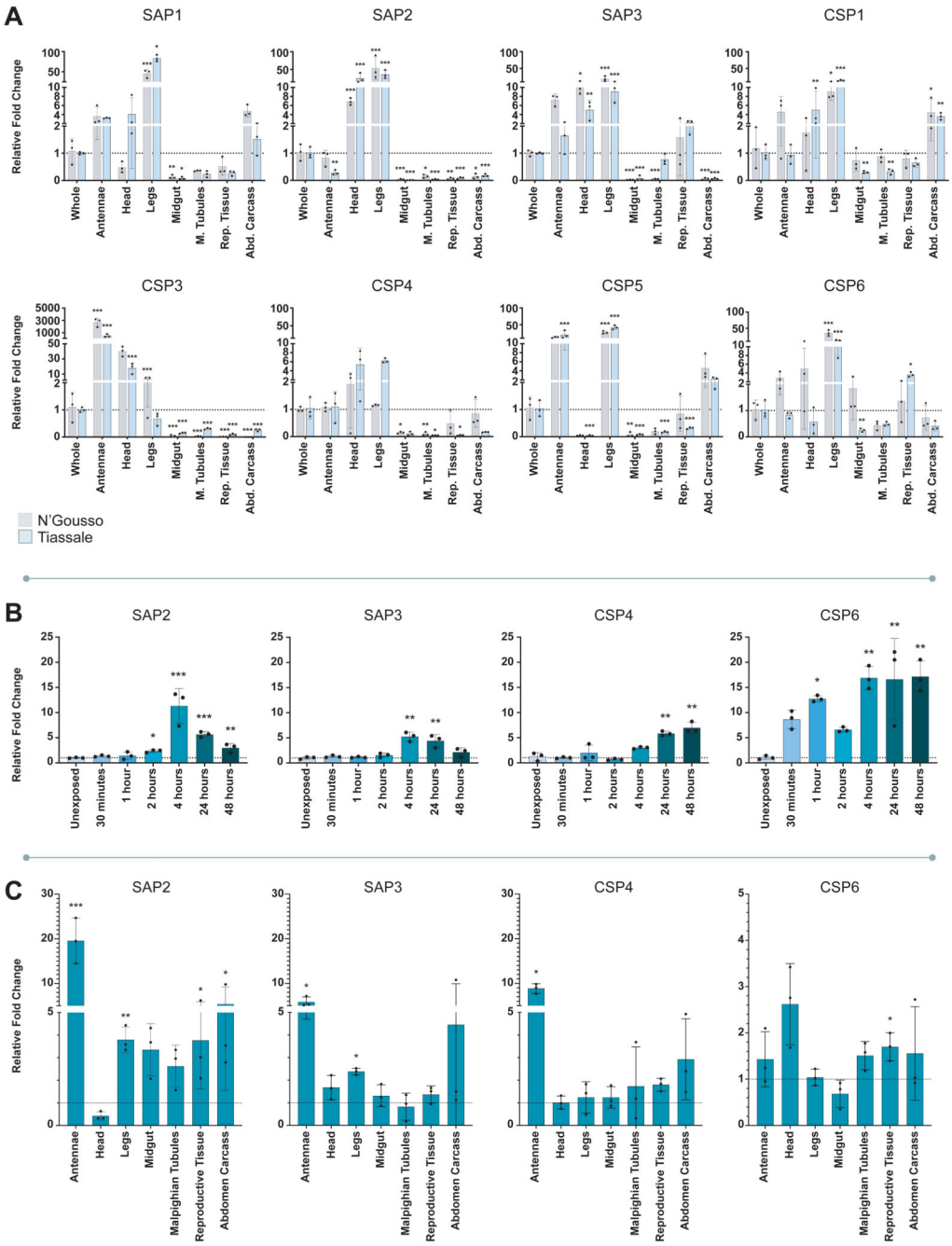

Figure 1. CSP expression profiles.

A. Constitutive expression of CSPs in resistant and susceptible strains. mRNA localisation in antennae, head, legs, midgut, Malpighian tubules, reproductive tissue and the remaining abdominal tissues (abdomen carcass) in N'Gousso (grey) and Tiassalé (blue) for each member of the CSP family compared to whole body. **B**. Induction of CSPs in Tiassalé following pyrethroid exposure. Four CSPs show significant induction of mRNA expression at different time points post-exposure to the pyrethroid insecticide deltamethrin in Tiassalé (results for the non-induced CSPs are shown in Extended Data Figure 3a). **C.** Tissue-specific

profile of CSPs induction in Tiassalé. Tissue-specific induction for the four significantly induced CSPs in the Tiassalé strain, shown 4-hours post deltamethrin exposure, each data point shows exposed compared to unexposed tissues from the same generation (see Extended Data Figure 3b for remaining CSPs). The qPCR data show mean ± standard deviation of three biological replicates. * $p \leq 0.05$; ** $p \leq 0.01$; *** $p \leq 0.001$. Statistical significance was calculated by an ANOVA followed by Dunnett's *post hoc* test; where normalisation was not possible, data was analysed using Kruskall-Wallis followed by a Dunn's *post hoc* test in **A.** and **B.** In **C.** significance was calculated by a two-tailed t-test; p-values are provided in Supplementary Table 2; n = 3 for each replicate.

Europe PMC Funders Author Manuscripts

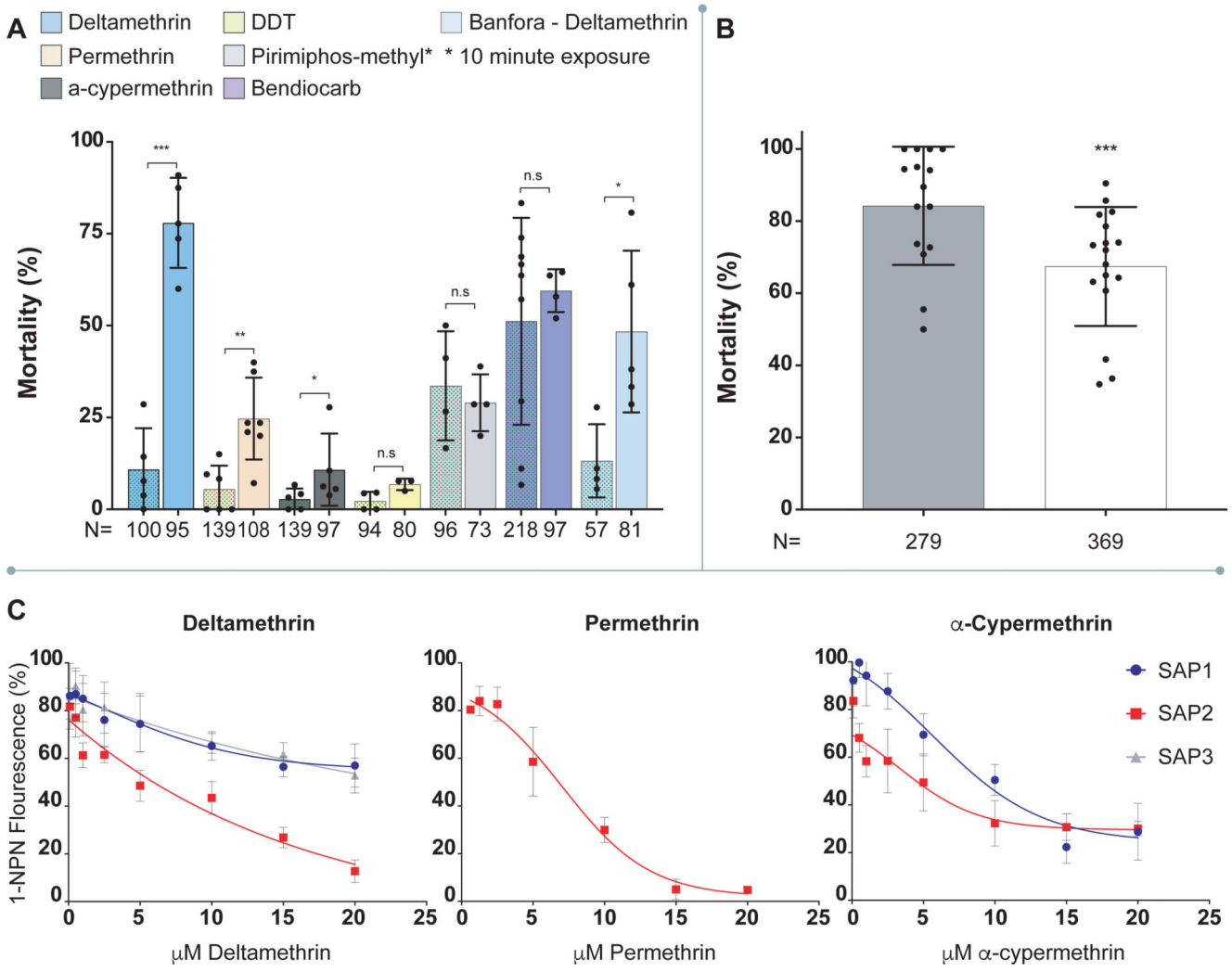

Figure 2. *SAP2* mediates resistance to pyrethroid insecticides.

A. Effect of *SAP2* knock down on mortality in multi-resistant *Anopheles* populations in response to a panel of insecticides (rightmost bar) compared to GFP-injected controls (leftmost bar; patterned). Tiassalé: Deltamethrin (blue; $n_{GFP;SAP2}$ = 5;5); Permethrin (pink; $n_{GFP;SAP2}$ = 6;7); α-cypermethrin (dark grey; $n_{GFP;SAP2}$ = 5;5); DDT (yellow; $n_{GFP;SAP2}$ = 4;3), primiphos-methyl (light grey; $n_{GFP;SAP2}$ = 4;4) and Bendiocarb (dark blue $n_{GFP;SAP2}$ = 9;4). Banfora: Deltamethrin (light blue; $n_{GFP;SAP2}$ = 4;5). N represents the total number of females used across all replicates. **B**. Transgenic over-expression of *SAP2* in susceptible G3 mosquitoes reduces mortality after permethrin exposure. Bars represent control (grey; n = 15) and *SAP2* overexpression (white; n = 17). N represents the total number of females used across all replicates. **C**. Competitive binding assays of the three SAP proteins to three pyrethroid insecticides. Only instances with binding shown; no binding for: *SAP3* nor *SAP1* with permethrin; *SAP3* with α-cypermethrin; any SAP with bendiocarb or pirimiphos-methyl. The data show mean ± standard deviation. * $p \leq 0.05$; ** $p \leq 0.01$; *** $p \leq 0.001$; ns $p > 0.05$. Statistical significance in 2A and 2B calculated by an ANOVA test followed by a Tukey *post hoc* test; p-values are provided in Supplementary Table 2

Europe PMC Funders Author Manuscripts

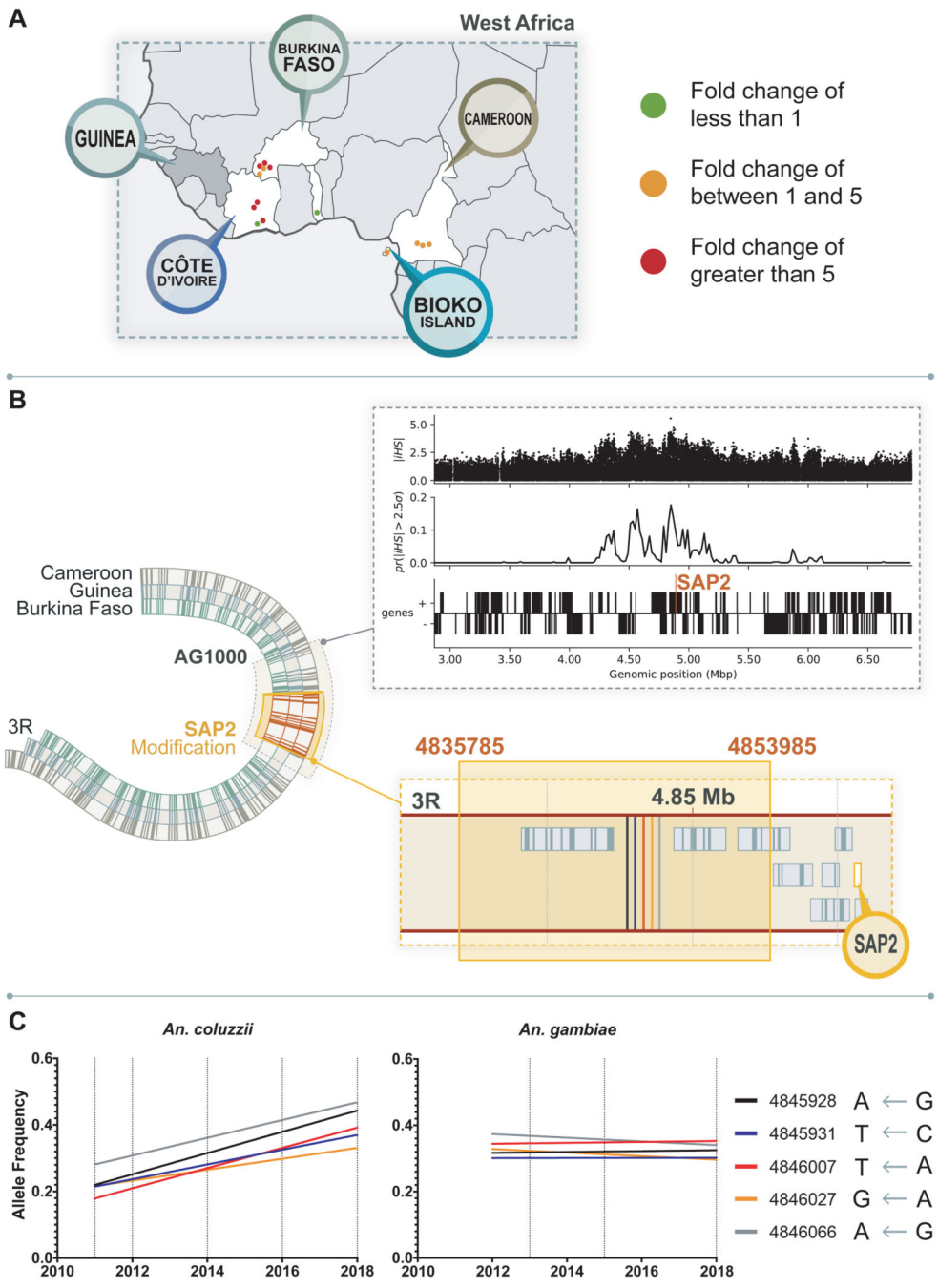

Figure 3. *SAP2* is up-regulated and under selection in multiple countries across West Africa.

A. Points represent significantly differential expression of *SAP2* in pyrethroid resistant mosquitoes in two sister species (*An. coluzzii* or *An. gambiae*) compared to susceptible populations (Extended Table 1, from [10]). Significant ($p_{limma;BH\text{-}corrected}$[10] ≤ 0.05) fold changes are represented by a traffic light system. Countries with *SAP2* either (i) significantly up-regulated and/or (ii) involved in the selective sweep are highlighted with a pin. No transcriptomic data is available for Guinea. Map created expressly for this manuscript by Manuela Bernardi. **B.** Schematic representation of the range of the selective

Europe PMC Funders Author Manuscripts

Europe PMC Funders Author Manuscripts

sweep found in Guinea, Burkina Faso and Cameroon with selective sweep found across these regions in the *Anopheles* 1000 genomes highlighted in grey [19]. Observed iHS signal from Guinea is shown as follows, from top to bottom panels: Raw iHS statistics per SNP, normalised by chromosome in allele frequency bins; summarised iHS in windows of 20kbp by proportion of SNPs exceeding 2.5 standard deviations [20]; and genes in this region with *SAP2* annotated. Highlighted in yellow are the range of the 55 SNPs tagging this haplotype across the three countries. A zoomed in area shows the approximate location of the five haplotype tagging SNPs in proximity to *SAP2* (more detail in Extended Data Figure 1A). **(C)** Fitted trend in frequency of the derived haplotype associated SNPs in field populations from Burkina Faso: (i) *An. coluzzii* populations collected from Tengrela from 2011 to 2018 and (ii) *An. gambiae* s.s. samples collected in 2013 and 2015 from Bakaridjan, Burkina Faso and 2018 from Tiefora, Burkina Faso. Dates when samples were sequenced are indicated by a dotted line. SNP data is shown in the legend, including the locus and the alternate allele (left) and PEST allele (right).